ChemComm

Binding selectivity and separation of p-functionalized toluenes with a metallo cavitand in water

Journal:	*ChemComm*
Manuscript ID	CC-COM-04-2020-002778.R1
Article Type:	Communication

COMMUNICATION

Binding selectivity and separation of *p*-functionalized toluenes with a metallo cavitand in water

Faiz-Ur Rahman,[a] Ji-min Yang,[c] Yunhui Wan,[a] Hui-bin Zhang,[a] Ioannis D. Petsalakis,[b] Giannoula Theodorakopoulos,[b] Julius Rebek Jr.,* [a, c] Yang Yu*[a]

Received 00th January 20xx,
Accepted 00th January 20xx

DOI: 10.1039/x0xx00000x

Metallo cavitand (1-2Pd) showed unprecedented binding selectivity and sequestration of *p*-functionalized toluene isomers in water. The host-guest complexation was studied by ^{1}H and COSY NMR methods and xylene-isomer complexes were examined by DFT calculations. A liquid-liquid extraction scheme was developed for separation of *p*-functionalized toluenes.

One of the recently identified "seven chemical separations to change the world"[1] is the efficient isolation of *p*-xylene from its *o*- and *m*- isomers. Their boiling points (BP) are close (ESI Table S1) and fractional distillation is energy consuming and difficult. Toluene as a substrate in reactions such as nitration, Friedel-Crafts alkylation, formylation or acetylation produces mixtures of isomers. The subtle differences in their BP's and polarities require laborious purification methods. Here we describe a supramolecular approach to such separations without the use of energy-intensive, expensive or hazardous procedures.

A number of methods have been proposed to meet the separation challenge, including application of MOF's[2, 3], COF's[4], membranes, solid absorption methods[5] and earlier techniques.[6] Approaches based on molecular recognition are scarce. A promising example involves pillararenes. In the crystalline state, open-ended pillar[5]arenes offer faster absorption of *p*-xylene based on its shape complementarity.[7] There appear to be no examples of liquid-liquid phase separation for *p*-xylene and related positional isomers of functionalized toluenes.

Cavitands with quinoxaline walls were introduced by Cram[8] who deduced that they can exist in two shapes: the unreceptive kite or velcrand form and the receptive vase form. Dalcanale[9] and Diederich[10-12] subsequently determined the effects of temperature, pH, solvent and metal ions on the equilibrium between the kite and vase forms of the classical, organic-soluble cavitands. Cavitands soluble in water include Gibb's[13-16] rigid containers and our[17-22] flexible ones. These cavitands were studied extensively in molecular recognition and as reaction vessels in water. Although molecular weight and size selectivity was reported in a few cases involving capsular assembly,[23-25] the containers were largely indiscriminate in recognizing isomers. Similarly, the recognition of the guests by a supramolecular host showed high dependency on solvent it dissolved.[26-29] Nonpolar or amphiphilic molecule guests showed good binding in cavitands in water, the hydrophobicity works as a main driving force that pushes guest molecule to a hydrophobic cavity formed by the cavitand nanostructures.[19, 30] We recently introduced a water-soluble cavitand **1**[31] and its Pd(II) derivative **1-2Pd** (Scheme 1).[32] The placement of metals rigidifies the cavity[33] and slows the dynamics of guest exchange.[34] The coordination stabilizes[35, 36] the receptive vase shapes and imparts a welcome selectivity in guest binding. The narrowed space of the host **1-2Pd** leads to general recognition of alkyl chains. Normal alkanes, alcohols and carboxylic acids are all bound in a linear fashion by their methyl "tails" and cyclic alkanes are also accomodated in the constricted, hydrophobic cavity.[32] We used the selective binding to isomeric aromatics to open a path to separation of *p*-functionalized toluenes from their isomers.

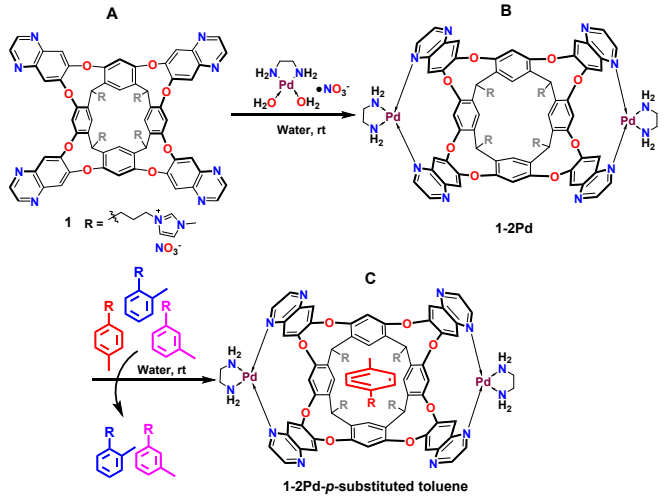

Scheme 1. Quinoxaline based cavitand **1** (A) bears imidazolium "feet" that impart

[a] Center for Supramolecular Chemistry & Catalysis and Department of Chemistry, College of Science, Shanghai University, 99 Shang-Da Road, Shanghai 200444, China
[b] Theoretical and Physical Chemistry Institute, The National Hellenic Research Foundation, 48 Vassileos Constantinou Ave. Athens 116 35, Greece
[c] Skaggs Institute for Chemical Biology and Department of Chemistry, The Scripps Research Institute, 10550 North Torrey Pines Road, La Jolla, CA 92037, USA
E-mail: jrebek@scripps.edu, yangyu2017@shu.edu.cn.
Electronic Supplementary Information (ESI) available: For ^{1}H NMR spectra and other related data see DOI: 10.1039/x0xx00000x

solubility in water. Its dimetallic Pd(II) complex **1-2Pd** (B) selectively binds *p*-functionalized toluenes (C) in competition with *o*- and *m*-isomers

Sonication of **1** in D_2O with any of the substitituted toluenes, mixtures of isomers or related compounds failed to disrupt the dimeric velcrand complex (velcraplex). No host/guest interactions were observed. But adding a Pd(II) precursor ([Pd(ethylene diamine)$(H_2O)_2$·2NO_3]) generated **1-2Pd** *in situ* which captured only the *p*-substituted toluenes (Scheme 1). The metal coordination occurs at two sites as shown, leading to a rhombus-like arrangement of the 4 walls and a "pinched cone" resorcinarene base.[37] All of the xylene guests showed sharp signals in their NMR spectra but with other functionalized toluenes only the *p*-isomer bound well (Figure 1A-B and ESI Figure S6-S8). The sharp signals in the spectra of different isomers allowed the interpretation of their orientations and motions in the cavitand. Experimentally, in case of *p*-xylene the rhomboidal arrangement of walls induces an upfield shift, Δδ = −5.5 ppm at the cavity's bottom and -3.1 ppm near its top, agreeing with computed values.[38] The higher and close quinoxaline walls and the pinched cone shape of the resorcinarene platform contribute to the sizable upfield shifts of the guest. For *p*-xylene, widely separated methyl signals indicate that it tumbles slowly on the NMR chemical shift timescale. Two upfield signals (the shoulder peak) indicate isomeric complexes with nearly the same magnetic environment of the deeper -CH_3 groups (ESI Figure S8). We propose two isomeric arrangements as shown (Figure 2A-B and ESI Figure S8), with slow interconversion between them. For *o*-xylene the favored arrangement (75%) has both methyls deep in the cavity and the less favored one (25%) has the methyls near the open end (Figure 2C-D and ESI Figure S6). The *m*-xylene guest shows only one signal for its methyl groups; this guest tumbles rapidly on the NMR timescale (Figure 2E-F and ESI Figure S7).

Competition experiments showed that *p*-xylene completely displaces the other isomers from their complexes (Figure 1B and ESI Figure S9-S13), and the selectivity was 100% for *p*-xylene when host:*p*-xylene: *o*- (or *m*-xylene or both) isomer ratios were 1:1:1.

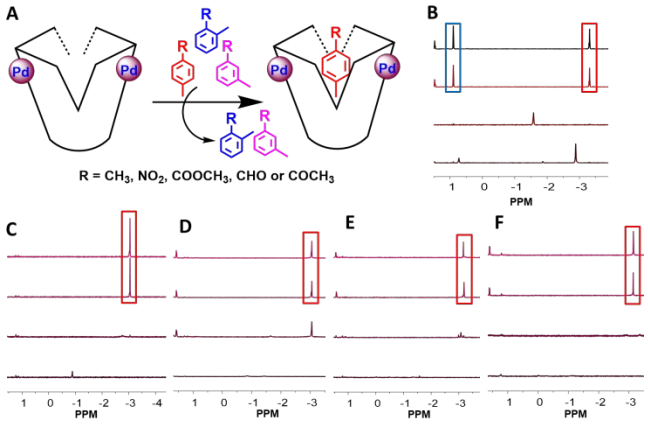

Figure 1. Binding selectivity of **1-2Pd** for functionalized toluene and partial ^{1}H NMR spectra (Panel B-F), 1 mM **1-2Pd** + excess of one isomer or mixture of isomers of particular guest, taken in D_2O (600 MHz, 298 K). A) Cartoon scheme showing **1-2Pd** capture of *p*-isomers from mixtures with exclusive selectivity. B) Xylene isomers; C) Nitro toluene isomers; D) Toluic acid ester isomers; E) Tolualdehyde isomers; F) Acetyltoluene isomers. The bottom trace is always *o*-, the next *m*-, the third *p*- and the top trace is *o*-, *m*-, *p*- isomers as 1:1:1 mixtures (the red rectangle shows the deeply bound methyl group while the blue rectangle shows the shallow methyl).

A mixture of xylenes, similar to that obtained from fossil fuel distillate fractions (20-25% *o*-xylene, 20-25% *p*-xylene and 50-60% *m*-xylene), in CD_3OD was used as a stock solution and added to **1-2Pd** in increments. The container again showed high selectivity for *p*-xylene (ESI Figure S20-S22).

Isomeric nitrotoluenes showed different binding; the *o*- and *m*-isomers did not show clean binding to deduce their orientation in the cavity, while the *p*-isomer bound well. From a mixture, only the *p*-isomer was taken in (Figure 1C and ESI Figure S23-S27). The methyl group of nitrotoluene was bound deep in the cavity while the NO_2 group occupied the opening, exposed to water.

The *o*-isomer of methyltoluate did not show binding (Figure 1D and ESI Figure S28-S32). The *m*- and *p*- isomers bound well and showed similarity in binding, but from a mixture of the two, only the *p*-isomer was taken in, as deduced from pattern of the cavitand's aromatic proton signals. The C-methyl group was buried deep in the cavity while O-methyl group was exposed to water. We did not locate upfield shift for $COOCH_3$ due to the overlap with the signals for the cavitand's "feet".

For *p*-tolualdehyde, the methyl group was again bound deep inside the cavity while the more hydrophilic CHO group was exposed to the open mouth (Figure 1E and ESI Figure S33-S37). The binding of *p*-acetyl toluene was similar (Figure 1F and ESI Figure S38-S42). In both of these compounds, the *o*- and *m*-isomers did not show detectable binding; the selectivity was exclusive and the *p*-isomer could be separated efficiently from a mixture using **1-2Pd**.

All of these functionalized toluene *p*-isomers showed an upfield shift, Δδ around −5.5 ppm for the methyl bound deep in the cavity and the relative integration of the host and guest showed 1:1 stoichiometry. Similarly, the change in chemical shifts (Δδ) for other aromatic protons of each *p*-functionalized toluene were analyzed by ^{1}H COSY NMR analysis (ESI Figure S5) and the values are tabulated in ESI Table S2.

Direct isothermal titration calorimetry (ITC) could not be used to obtain binding constants as the xylenes are insufficiently water-soluble. Instead, we used *n*-butanol as a reference guest and observed 1:1 complex formation with a binding constant $K = 1.54 \times 10^5$ M^{-1} by ITC (ESI Figure S43). Direct competition of *n*-butanol with xylenes using ^{1}H NMR spectroscopy showed the alcohol has a higher binding constant than *o*- and *m*-xylene but is comparable to *p*-xylene (ESI Figure S43-S53).

Geometry-optimization DFT calculations[39] were carried out on different conformations of *ortho*, *meta* and *para*-xylene bound in the **1-2Pd** (with modified feet) as a reference for toluene derivatives. The M062X functional[40, 41] was employed along with the Lanl2dz basis set.[42, 43] We have found these calculations accurately predict binding preferences for related container compounds and their guests.[23, 32] The lowest energy optimized structures for **1-2Pd** and with *p*-xylene in the cavity are displayed in Figure 2A-B. These structures exemplify the two types of orientations found for the different local minima of the

p-xylene, *m*-xylene and *o*-xylene complexes, with the lowest energy structures indicated in Figure 2A-F NMR shifts were obtained using the Gauge-Independent Atomic Orbital (GIAO) method.[44] The results are summarized in the ESI Figures S1-S4.

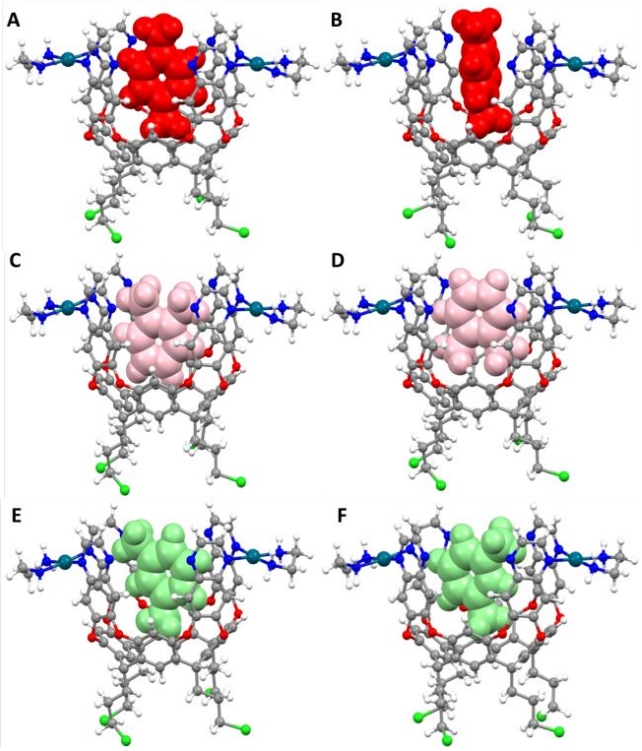

Figure 2 Computed structures of the xylene complexes with **1-2Pd**. (A) and (B): *p*-Xylene in two low-energy orientations in the cavitand. Interconversion between complexes by guest rotation and tumbling is slow on the NMR timescale, and separate signals are seen for the methyl groups. (C) and (D): Isomeric arrangements of *o*-xylene; again, tumbling is slow. (E) and (F): *m*-Xylene mirror image isomers interconvert rapidly through a proposed tumbling motion that exchanges environments of the methyl groups.

The liquid phase separation scheme is shown in Figure 3A that was applied to *p*-xylene separation from other isomers. As mesitylene is a bad guest and it could not bind in **1-2Pd** in the presence of even a small amount *p*-xylene (ESI Figure S56), therefore we initially used a mesitylene solution of *p*-xylene only and successfully determined the recyclability of the host and also quantified the recovered amount of bound *p*-xylene form aqueous solution of **1-2Pd**. (ESI Figure S54-S62). We also applied the binding selectivity to the separation of a typical mixture of xylene isomers obtained from crude oil distillation (1:3:1 *o*-:*m*-:*p*-isomers). When xylene isomers mixture was suspended in a solution of **1-2Pd** in D_2O, *p*-xylene can be recognized (Figure 3B) by the **1-2Pd** host and transferred into the aqueous solution, leaving the other two isomers in organic phase (Figure 3C and ESI Figure S63-S65). The bound *p*-xylene was extracted from the aqueous solution by using an organic solvent such as chloroform (Figure 3C and ESI Figure S56-S65), ethyl acetate (ESI Figure S66-S68) or dichloromethane (ESI Figure S69-S72). The extracted *p*-xylene quantity was determined using DMSO as internal standard which showed the 100 % recovery of *p*-xylene based on the concentration of the host (ESI Figure S65). The aqueous solution of the **1-2Pd** can be reused to perform another cycle. The binding and liquid-liquid extraction of xylene mixture using **1-2Pd** was quantified and the recyclability of this supramolecular host system was confirmed by different approaches discussed in the ESI (Figure 3A and ESI Figure S54-S72). This isomeric guests separation process (Figure 3A and Figure ESI S73) was also applied to the separation of *p*-nitrotoluene from its isomers (ESI Figure S74-S77).

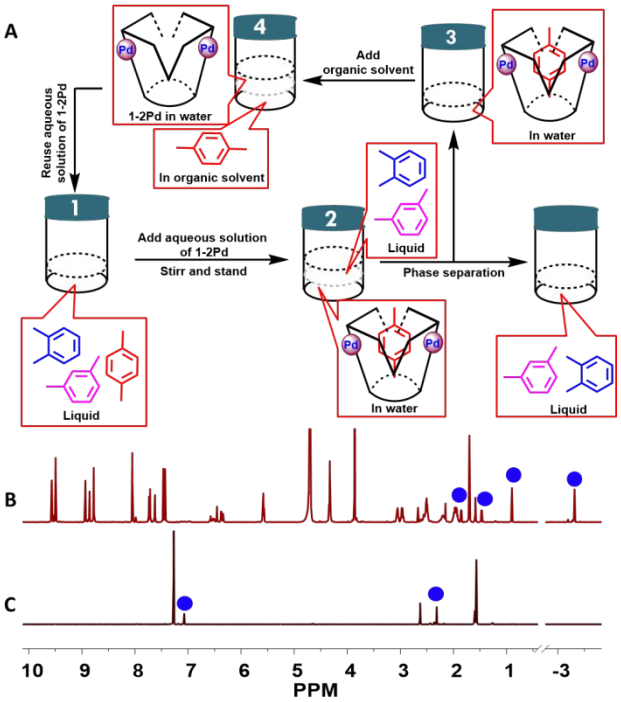

Figure 3. (A) General liquid-liquid separation scheme for *p*-xylene and (B, C) partial ^{1}HNMR spectra (600 MHz, 298 K). (B) The aqueous (D_2O) phase 3 was *p*-xylene ☐ **1-2d**, (Blue circles showed ^{1}H chemical shifts of *p*-xylene bound in **1-2Pd**); (C) The organic phase ($CDCl_3$) extracted in step 4 showing *p*-xylene extracted from water phase (blue circles showed the ^{1}H chemical shifts of *p*-xylene.

In summary, we established that **1-2Pd** in water is a selective container for *p*-functionalized toluene derivatives. We applied this supramolecular system in liquid-liquid extraction processes to separate *p*- from their *o*- and *m*- isomers. While we can hardly recommend the stoichiometric use of a Pd-fretted container for separating a bulk commodity like xylene, this is a first step in developing a method that could be used for environmentally benign or cost effective separation of such closely related isomers. The choice of Pd was based on its NMR compatibility; other, cheaper metal ions should serve the same purpose for reorganizing the cavity in water. The current liquid/liquid extraction experiments also augur well for a process involving a transport system such as in a U-tube[27, 45] for the use of the cavitand in a continuous, catalytic sense or supported in a membrane.[46] We are exploring these possibilities.

This work was supported by the National Natural Science Foundation of China (Grant No. 21801164), the US National Science Foundation (CHE 1801153) and by Shanghai University (N.13-G210-19-230), Shanghai, China. Dr. Yang Yu thanks the Program for Professor of Special Appointment (Dongfang Scholarship) of the Shanghai Education Committee.

Conflicts of interest

There are no conflicts to declare.

Notes and references

1. D. S. Sholl and R. P. Lively, *Nature*, 2016, **532**, 435-437.
2. M. I. Gonzalez, M. T. Kapelewski, E. D. Bloch, P. J. Milner, D. A. Reed, M. R. Hudson, J. A. Mason, G. Barin, C. M. Brown and J. R. Long, *J. Am. Chem. Soc.*, 2018, **140**, 3412-3422.
3. W. Huang, J. Jiang, D. Wu, J. Xu, B. Xue and A. M. Kirillov, *Inorg. Chem.*, 2015, **54**, 10524-10526.
4. J. Huang, X. Han, S. Yang, Y. Cao, C. Yuan, Y. Liu, J. Wang and Y. Cui, *J. Am. Chem. Soc.*, 2019, **141**, 8996-9003.
5. S. Q. Wang, S. Mukherjee, E. Patyk-Kazmierczak, S. Darwish, A. Bajpai, Q. Y. Yang and M. J. Zaworotko, *Angew. Chem. Int. Ed. Engl.*, 2019, **58**, 6630-6634.
6. Y. Yang, P. Bai and X. Guo, *Ind. Eng. Chem. Res.*, 2017, **56**, 14725-14753.
7. K. Jie, M. Liu, Y. Zhou, M. A. Little, A. Pulido, S. Y. Chong, A. Stephenson, A. R. Hughes, F. Sakakibara, T. Ogoshi, F. Blanc, G. M. Day, F. Huang and A. I. Cooper, *J. Am. Chem. Soc.*, 2018, **140**, 6921-6930.
8. J. R. Moran, S. Karbach and D. J. Cram, *J. Am. Chem. Soc.*, 1982, **104**, 5826-5828.
9. E. Dalcanale, P. Soncini, G. Bacchilega and F. Ugozzoli, *J. Chem. Soc., Chem. Commun.*, 1989, 500-502.
10. P. J. Skinner, A. G. Cheetham, A. Beeby, V. Gramlich and F. Diederich, *Helv. Chim. Acta*, 2001, **84**, 2146-2153.
11. V. A. Azov, B. Jaun and F. Diederich, *Helv. Chim. Acta*, 2004, **87**, 449-462.
12. M. Frei, F. Marotti and F. Diederich, *Chem. Commun.*, 2004, 1362-1363.
13. S. Liu and B. C. Gibb, *Chem. Commun.*, 2008, DOI: 10.1039/b805446k, 3709-3716.
14. J. H. Jordan and B. C. Gibb, *Chem. Soc. Rev.*, 2015, **44**, 547-585.
15. J. Murray, K. Kim, T. Ogoshi, W. Yao and B. C. Gibb, *Chem. Soc. Rev.*, 2017, **46**, 2479-2496.
16. K. Wang, X. Cai, W. Yao, D. Tang, R. Kataria, H. S. Ashbaugh, L. D. Byers and B. C. Gibb, *J. Am. Chem. Soc.*, 2019, **141**, 6740-6747.
17. D. Ajami and J. Rebek, Jr., *Acc. Chem. Res.*, 2013, **46**, 990-999.
18. Y. Yu and J. Rebek, Jr., *Acc. Chem. Res.*, 2018, **51**, 3031-3040.
19. K. D. Zhang, D. Ajami, J. V. Gavette and J. Rebek, Jr., *Chem Commun (Camb)*, 2014, **50**, 4895-4897.
20. R. J. Hooley, H. J. Van Anda and J. Rebek, Jr., *J. Am. Chem. Soc.*, 2007, **129**, 13464-13473.
21. K. D. Zhang, D. Ajami, J. V. Gavette and J. Rebek, Jr., *J. Am. Chem. Soc.*, 2014, **136**, 5264-5266.
22. K. D. Zhang, D. Ajami and J. Rebek, *J. Am. Chem. Soc.*, 2013, **135**, 18064-18066.
23. F. U. Rahman, D. Tzeli, I. D. Petsalakis, G. Theodorakopoulos, P. Ballester, J. Rebek, Jr. and Y. Yu, *J. Am. Chem. Soc.*, 2020, **142**, 5876-5883.
24. C. L. Gibb and B. C. Gibb, *J. Am. Chem. Soc.*, 2006, **128**, 16498-16499.
25. S. Liu, H. Gan, A. T. Hermann, S. W. Rick and B. C. Gibb, *Nat Chem*, 2010, **2**, 847-852.
26. F. N. Diederich, *Cyclophanes*, The Royal Society of Chemistry, Cambridge CB4 4WF 1991.
27. F. Diederich and K. Dick, *J. Am. Chem. Soc.*, 1984, **106**, 8024-8036.
28. J. L. Bolliger, T. K. Ronson, M. Ogawa and J. R. Nitschke, *J. Am. Chem. Soc.*, 2014, **136**, 14545-14553.
29. H. J. Schneider, R. Kramer, S. Simova and U. Schneider, *J. Am. Chem. Soc.*, 1988, **110**, 6442-6448.
30. Y. Yu, Y.-S. Li and J. Rebek, *New J. Chem.*, 2018, **42**, 9945-9948.
31. F.-U. Rahman, H.-N. Feng and Y. Yu, *Org Chem Front*, 2019, **6**, 998-1001.
32. F. U. Rahman, Y. S. Li, I. D. Petsalakis, G. Theodorakopoulos, J. Rebek, Jr. and Y. Yu, *Proc Natl Acad Sci U S A*, 2019, **116**, 17648-17653.
33. S. Korom and P. Ballester, *J. Am. Chem. Soc.*, 2017, **139**, 12109-12112.
34. L. Escobar, D. Villaron, E. C. Escudero-Adan and P. Ballester, *Chem. Commun.*, 2019, **55**, 604-607.
35. P. Roncucci, L. Pirondini, G. Paderni, C. Massera, E. Dalcanale, V. A. Azov and F. Diederich, *Chem. Eur. J.*, 2006, **12**, 4775-4784.
36. T. Iwasawa, *Tetrahedron Lett.*, 2017, **58**, 4217-4226.
37. M. Conner, V. Janout and S. L. Regen, *J. Am. Chem. Soc.*, 1991, **113**, 9670-9671.
38. P. V. R. Schleyer, C. Maerker, A. Dransfeld, H. Jiao and N. J. R. van Eikema Hommes, *J. Am. Chem. Soc.*, 1996, **118**, 6317-6318.
39. A. D. Becke, *J. Chem. Phys.*, 1993, **98**, 5648-5652.
40. Y. Zhao and D. G. Truhlar, *Theor. Chem. Acc.*, 2007, **120**, 215-241.
41. Y. Zhao and D. G. Truhlar, *Acc. Chem. Res.*, 2008, **41**, 157-167.
42. , T. H. Dunning Jr. and P. J. Hay, in Modern Theoretical Chemistry, Ed. H. F. Schaefer III, Vol. 3 (Plenum, New York, 1977) 1971-1928. .
43. W. R. Wadt and P. J. Hay, *J. Chem. Phys.*, 1985, **82**, 284-298.
44. K. Wolinski, J. F. Hinton and P. Pulay, *J. Am. Chem. Soc.*, 1990, **112**, 8251-8260.
45. B.-L. Poh and Y. M. Chow, *J. Inclusion Phenom. Mol. Recognit. Chem.*, 1992, **14**, 85-90.
46. M. du Plessis, V. I. Nikolayenko and L. J. Barbour, *J. Am. Chem. Soc.*, 2020, DOI: 10.1021/jacs.9b11314.